

Conodont biostratigraphy and faunal assemblages in radiolarian ribbon-banded cherts of the Burubaital Formation, West Balkhash Region, Kazakhstan

TATIANA TOLMACHEVA*†, LARS HOLMER*, LEONID POPOV‡ & IVAN GOGIN§

*Department of Earth Sciences, Palaeobiology, Uppsala University, Norbyvägen 22, SE-75236, Uppsala, Sweden

‡Department of Geology, National Museum and Galleries of Wales, Cathays Park, Cardiff CF10 3NP, United Kingdom

§Department of Stratigraphy and Palaeontology, All Russian Scientific Research Geological Institute (VSEGEI), Sredny 74, St. Petersburg, Russia

(Received 13 February 2003; revised version received 25 May 2004; accepted 17 June 2004)

Abstract – Biostratigraphical study of the early to mid-Ordovician conodont fauna from ribbon-banded radiolarian cherts of the middle Burubaital Formation in Central Kazakhstan reveals an almost complete succession of conodont biozones from the late Tremadocian to the early Darriwilian. During this interval, biosiliceous sediments were deposited in basinal environments, inhabited by lingulate brachiopods, sponges, pterobranchs and caryocaridids in conditions of high fertility and primary productivity of surface water. The community structure of taxonomically diverse conodont assemblages typifying open oceanic environments is not significantly different from that of epicratonic basins of the North Atlantic conodont province. The regional increase of oxygenated bottom waters at the base of the *Oepikodus evae* Biozone is possibly related to considerable changes in palaeo-oceanographical circulation patterns. The finds of three natural clusters of *Prioniodus oepiki* (McTavish) enable us to propose an emended diagnosis of this species.

Keywords: radiolarites, Conodonta, Kazakhstan, Ordovician.

1. Introduction

Current knowledge of conodont assemblages inhabiting Ordovician oceans remains inadequate, despite the fact that the occurrence of Ordovician conodonts in pelagic sediments deposited in oceanic environments, such as siliceous shales and radiolarian cherts associated with ophiolites, was first reported almost half a century ago (Lamont & Lindström, 1958).

The occurrence of conodonts in Ordovician radiolarian cherts and jaspers of Central Kazakhstan was first reported in the mid-1970s (Gridina & Mashkova, 1975). Before this pioneering study, the age of the Lower Palaeozoic radiolarian cherts in Kazakhstan was interpreted across a wide stratigraphical spectrum from the Precambrian to Silurian (e.g. Antonyuk, 1974; Tokmacheva, Kuznechevskii & Paletch, 1974). Subsequent studies during the last three decades reveal that conodonts are widespread in siliceous deposits associated with early Palaeozoic ophiolites in Central Kazakhstan (for review see Nikitin, 2002).

Most previous studies of conodonts from Ordovician cherts in Central Kazakhstan were based on finds from isolated localities (Nikitin, Apollonov & Tsay, 1980;

Nikitin *et al.* 1980; Kurkovskaya, 1985; Novikova, Gerasimova & Dubinina, 1983; Dvoichenko & Abaimova, 1987). In this region, early Palaeozoic biogenic siliceous deposits underwent extensive tectonic deformation and were included in tectonic melanges. Fragments of continuous stratigraphical sequences preserved in individual olistoliths do not usually exceed 10–15 m in thickness, and cover stratigraphical intervals corresponding to parts of one to three successive conodont biozones. The only known exceptions are relatively continuous conodont sequences from the early Arenig to early Llanvirn Ushkyzyl Formation in the Chingiz Range described by Zhylkaidarov (1998), and from the late Cambrian to middle Ordovician Burubaital Formation of the West Balkhash Region (Koren *et al.* 1993; Tolmacheva, Danelian & Popov, 2001).

Conodont biozonation of the Burubaital Formation is based on a succession of conodont assemblages obtained from two large olistoliths exposed about 4 km west of the southwestern coast of Lake Balkhash and northwest of the Burubaital railway station (Fig. 1). Preliminary reports on the conodont biostratigraphy of the lower part of this sequence from the Upper Cambrian *Eoconodontus notchpeakensis* Biozone to the Lower Ordovician *Paroistodus proteus* Biozone, with faunal logs, were published by Popov & Tolmacheva (1995) and Tolmacheva, Danelian & Popov (2001).

† Address for correspondence: Department of Stratigraphy & Palaeontology, All Russian Scientific Research Geological Institute (VSEGEI), Sredny 74, St Petersburg, Russia; e-mail: Tatiana.Tolmacheva@vsegei.ru



Figure 1. Schematic map of the western part of the West Balkhash Region, southern Central Kazakhstan, with a square indicating the locality 9706.

Here we present new data on the conodont sequence of the middle part of the Burubaital Formation within the stratigraphical interval from the uppermost Tremadocian to the lower Darriwilian.

2. Location and geological settings

Ribbon-banded cherts of the Burubaital Formation comprise part of a subduction–accretion complex formed during the Early to Late Ordovician times along the northeastern active margin of the early Palaeozoic terrane known as the Chu–Ili plate (Popov, Cocks & Nikitin, 2002). These cherts are situated within a number of nappes and are incorporated within a tectonic melange in a narrow belt known as the Burultas or Buruntau Tectonofacies Belt (Holmer *et al.* 2001), about 30–40 km wide, which is traceable for about 400 km from the upper reaches of the Sarysu river in the northern Betpak–Dala desert northwestwards to the southwestern coast of Lake Balkhash. Further southeast the Lower Palaeozoic rocks are beneath a Mesozoic–Cainozoic cover, but their presence is documented from a borehole core near the town of Kolshengil, about 150 km southwest of the outcrop area, where radiolarian cherts with Lower Ordovician conodonts were recovered (Koren *et al.* 1993). The Burubaital Formation consists exclusively of black and red ribbon-banded radiolarian cherts with a very low content of

siliciclastic and volcanic material. This confirms their sedimentation in open ocean environments far from any significant sources of fine siliciclastic and volcanic material (Apollonov, 2000; Tolmacheva, Danelian & Popov, 2001). Despite some reports (Nikitin, 2002), the stratigraphical contacts of the Burubaital Formation with underlying and overlying deposits are not yet clear.

Our studied section (L. 9706) of the Burubaital Formation, 54 m thick in total, is exposed continuously along both sides of an unnamed gorge crossing the northern slope of a ridge (45°02'11" N, 73°56'27" E) (Figs 1, 2). It consists exclusively of ribbon-banded radiolarian cherts dipping steeply towards the southwest (75–90°). Despite the presence of several thin beds of fine siliceous breccia there is no biostratigraphical evidence for extensive discontinuities that might exceed the duration of one conodont zone within the section (Fig. 3).

The exposed part of the Burubaital Formation can be subdivided into four informal lithostratigraphical units described below in ascending order (Figs 3, 4):

Unit 1 (0–5.3 m). This unit is composed of thin-bedded cherts with individual beds varying from 1 to 5 cm in thickness, predominantly grey with a few beds of red or pink chert. A single unit of black chert up to 1.5 cm thick crops out about 2.2 m above the base and a bed of breccia is present at the top of the unit. Four samples collected from the intervals 0.3 m, 0.7 m, 1.5 m and 4.0 m from the base of the unit contain numerous conodont elements, rare sponge spicules and fragments of pterobranch colonies. Dark grey and black cherts in the lower part of the section include small pyrite and apatite crystals and diffused organic matter distributed unevenly within the bed accentuating the fine lamination. Conodont elements are often fused into coprolite clusters usually containing 2 to 19 elements. Clusters composed of relatively large, adult elements usually contain lesser numbers of elements than clusters formed by juvenile elements.

Unit 2 (5.3–17.6 m). Thin-bedded red cherts with individual beds about 1–2 cm thick and a few beds of dark grey chert up to 7 cm thick comprise this unit. Thickness of individual beds increases towards the top of the unit. Two beds of siliceous breccia are present about 12.7 m from the base and at the top of the unit. Four samples (9 m, 14.8 m, 16.0 m and 16.6 m) within this interval show high concentration of conodont elements in the rock (up to 30 elements per 10 cm²) and distinct orientation along the bedding surfaces. Clusters of conodont elements are relatively common.

Unit 3 (17.6–20.8 m). This unit is composed of alternating red and grey bedded cherts with individual beds varying from 5 to 10 cm thick with some beds more than 10 cm thick. Numerous conodonts sampled from 18 m, 19 m, 19.1 m and 20.3 m are preserved exclusively as isolated elements. The associated fauna is represented by organophosphatic brachiopods, sponge



Figure 2. View of ribbon-banded radiolarian cherts in the middle part of the section 9706 (27–32 m). Scale bar is 1 metre in length.

spicules and numerous fragments of caryocaridid carapaces and pterobranch colonies.

Unit 4 (20.8–54 m). Bedded, opaque or semi-translucent, red and yellow cherts comprise this unit. Individual beds are usually 3–5 cm thick with concentrations of argillaceous material on uneven bedding surfaces. Fine clastic material is concentrated on bedding surfaces of thin beds of siliceous shale, rather than within the chert beds. A bed of fine siliceous breccia about 0.5 m thick is present at 10 m above the base of the unit. Conodonts were sampled from intervals of 23 m, 25.1 m, 27.5 m, 32 m, 33.3 m, 40.5 m, 41.2 m, 45.4 m, 52 m and 54 m. They occur exclusively as isolated, chaotically oriented elements. Obscure spots and worm-like structures expressed by differential recrystallization of silica, and the pattern of uneven distribution of colours observed in thin sections are interpreted as trace fossils.

3. Material and methods

The distribution of conodonts through the section is highly variable; some chert beds yield numerous conodont elements, which are easily visible through a hand lens, whereas others are almost barren. Conodonts and brachiopods are usually preserved as moulds or replaced by silica. Only a few conodont elements from black and dark grey cherts in the lowermost unit of

the section contain primary phosphatic matter. This kind of preservation makes the traditional technique of conodont extraction from cherts by hydrofluoric acid (Aitchison, 1998; Zhylkaidarov, 1998) impracticable. Therefore the conodonts were studied in thin sections approximately 0.5 mm thick. A total of 23 conodont samples were collected from the most fossiliferous levels determined in the field, and more than 400 thin sections were made.

The microscopic study of conodonts and other fossils was performed using a Nikon SMZ800 microscope. All fossils were photographed in transmitted and reflected light with a Nikon COOLPIX 990 digital camera. Figured specimens (Figs 5, 6, 7, 9) are housed in the Central Research Geological Exploration Museum (prefixed CNIGR Museum), St Petersburg, Russia (collection 12829).

4. Conodonts and conodont biozonation

At present, conodonts are the only fossils from the Burubaital Formation that are useful for biostratigraphical purposes. Their abundance varies significantly through the studied sequence from several tens of elements per 10 cm² to a single element per sample or complete absence. It is likely that the abundance of conodont elements is strongly affected by the degree of dissolution and secondary recrystallization of

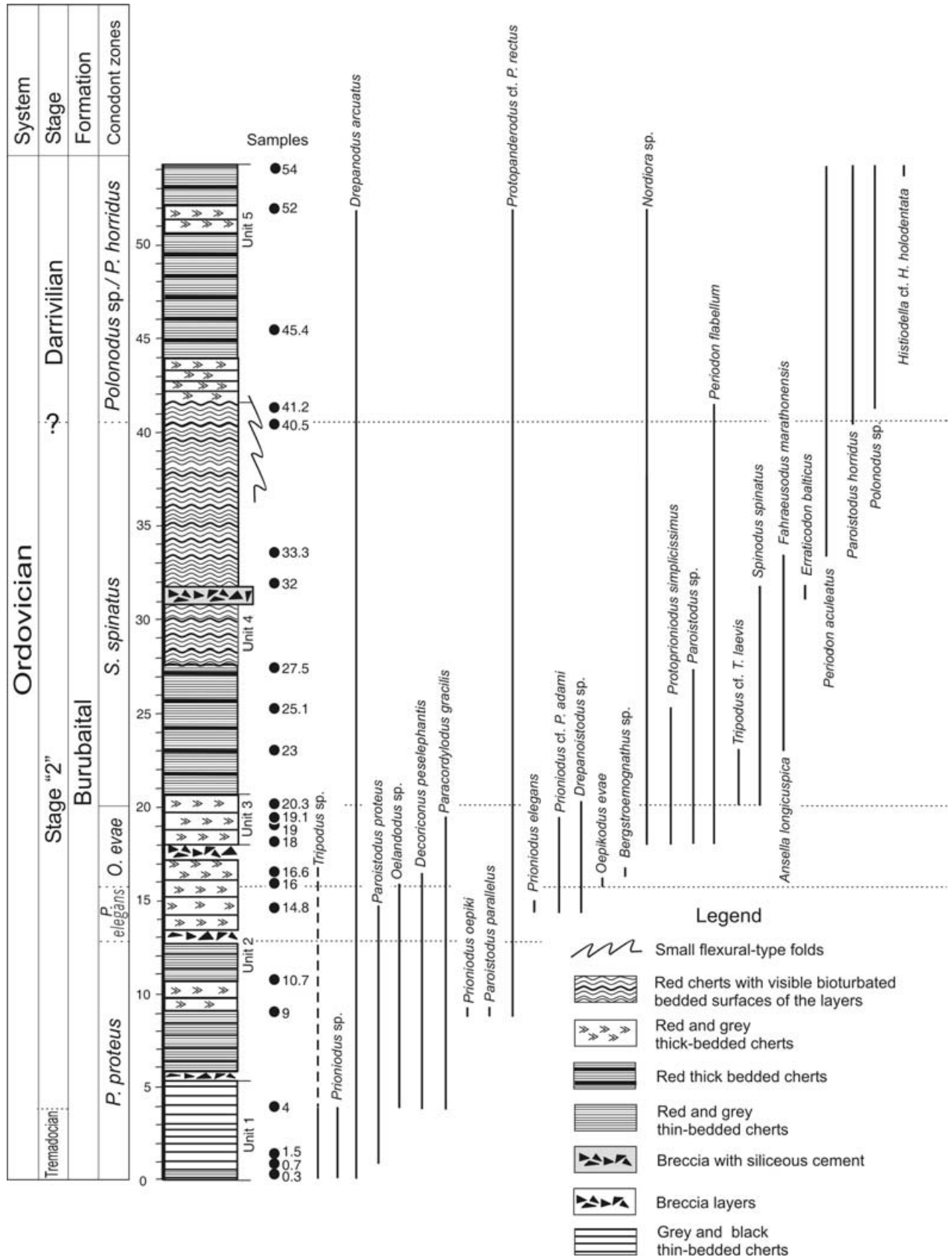


Figure 3. The stratigraphical column of the Burubaital Formation in the section 9706 showing sampled levels and stratigraphical ranges of conodonts.

Sample	Tripodus sp.	Drepanodus arcuatus	Prioniodus sp.	Paroistodus proteus	Oelandodus sp.	Paracordylodus gracilis	Decoriconus peselephantus	Prioniodus oepiki	Paroistodus parallelus	Protopanderodus cf. P. rectus	Drepanoistodus sp.	Prioniodus elegans	Prioniodus cf. P. adami	Oepikodus evae	Bergstroemognathus sp.	Nordlora sp.	Paroistodus sp.	Periodon flabellum	Protoprioniodus simplicissimus	Spinodus spinatus	Tripodus cf. T. laevis	Fahraeusodus marathonsensis	Ansella longicuspica	Erraticodon balticus	Paroistodus horridus	Periodon aculeatus	Polonodus sp.	Histiodella cf. H. holodentata	Unidentified species	Total			
9706-54 m																															10	0	10
9706-52 m	3									2						5							5	2	24	4	1	1	1	1	47		
9706-45.4 m				<i>Polonodus sp./ P. horridus</i>																									3	0	3		
9706-41.2 m										1								5					4	5	12	2				0	29		
9706-40.5 m	2									2								6					4	5	1				0	20			
9706-33.3 m																		9				6				4			0	19			
9706-32 m		<i>S. spinatus Zone</i>								1								13	2		21	4	2						0	43			
9706-27.5 m																3	2	85						3						0	93		
9706-25.1 m										1								100	2	8										2	113		
9706-23 m	10																1	250	5		1	2							2	271			
9706-20.3 m	8									1	5						4	3	200	2	12								2	237			
9706-19.1 m	10				1					2	1	5					5	190											2	216			
9706-19 m	32				15					4							4	400	1										2	458			
9706-18 m	4				4				2			6				1	6	74	1			<i>O. evae Zone</i>						1	99				
9706-16.6 m	1	6		8	100	1									1														0	117			
9706-16 m	2				43	4			1			1	4																0	55			
9706-14.8 m	8	1		70	2				2	2	1	3						<i>P. elegans Zone</i>						3	92								
9706-10.7 m	1				12																								0	13			
9706-9 m	15	2	3		6	45	30	3																					3	107			
9706-4 m	1	16	2	5	4	500	10										<i>P. proteus</i>										2	540					
9706-1.5 m	2	3	4																										1	10			
9706-0.7 m	3	1	1																										3	8			
9706-0.3 m	2	1	1																										4	8			

Figure 4. Numerical distribution of conodonts through the section.

biogenic apatite and silica within the host rock. Light-coloured grey and white cherts commonly lack sponge spicules and radiolarians, and contain poorly visible, shadow-like conodonts, which disappear completely in the proximity of more recrystallized areas around microcracks. The abundance of conodont elements also shows significant variation in similar chert lithologies, probably indicating fluctuations in sedimentation rate at particular stratigraphical intervals. Most of the samples are poor in conodonts and, except for a few dominant species, are represented by a small number of specimens, which makes their precise taxonomic discrimination difficult.

Taxonomic identification of conodont elements in cherts of the Burubaital Formation is difficult as they are usually available for observation only in lateral view. The proportions of juvenile elements in conodont assemblages from cherts are usually higher than those from the carbonate samples (Tolmacheva & Löfgren, 2000); in fact, the majority of conodont elements observed in the studied thin sections are juvenile. This also makes species identification questionable. Although the most common species have been identified, some rare species are recognizable at generic level only, or are almost unidentifiable.

The composition of conodont assemblages of the Burubaital Formation reveals a close similarity with contemporaneous Early to Middle Ordovician conodont faunas of Baltoscandia (Löfgren, 1978; Rasmussen, 2001), South-Central China (Zhang, 1998) and other regions located at that time in temperate latitudes, or deposited in relatively deep-water environments (Fig. 3). However, a considerable number of yet undescribed endemic species also occur.

Four biostratigraphical units can be recognized in the section (Figs 3, 4), described below in ascending order.

4.a. *Paroistodus proteus* Biozone

Three lowermost samples (0.3 m, 0.7 m and 1.5 m) yield *Paroistodus proteus* (Lindström), *Tripodus* sp., *Drepanodus arcuatus* Pander and *Prioniodus* sp. The latter is represented by a few weakly denticulate S elements and cannot be identified to species level. Abundance of conodont elements through this interval is very low and it is probable that the listed taxa do not represent the complete diversity of the fauna.

By contrast, the next sample (4 m) is extremely rich in conodonts, with *Paracordylodus gracilis* Lindström as a dominant taxon (up to 93 % of total number of

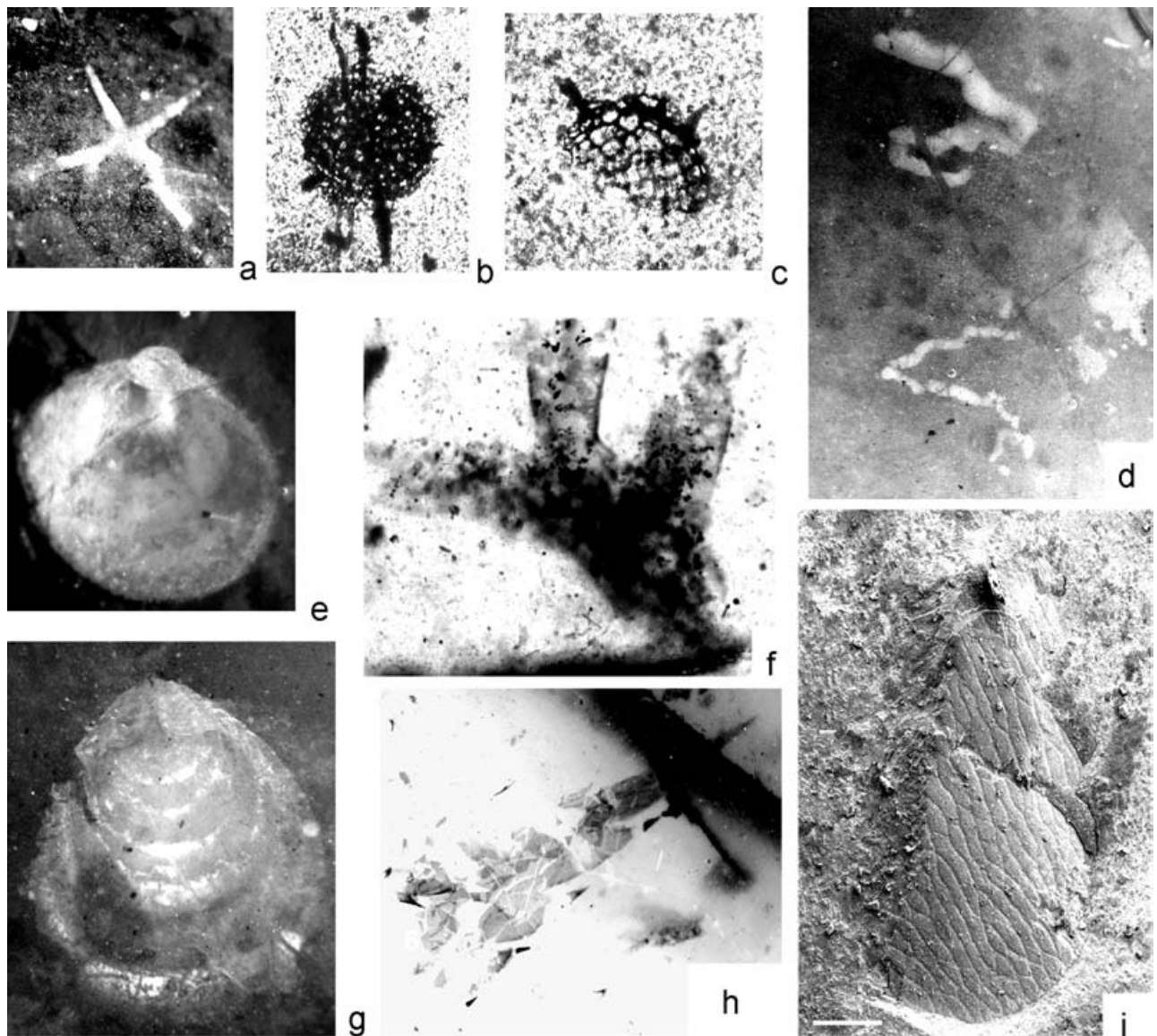


Figure 5. Photomicrographs of thin sections showing fossils from the section 9706. (a) Sponge spicule, incident light, sample 9706-32 m, *S. spinatus* Zone, $\times 25$, 12829/1. (b) Pyritized radiolaria, transmitted light, sample 9706-54 m, *Polonodus* sp./*P. horridus* Zone, $\times 120$, 12829/2. (c) Pyritized radiolaria, transmitted light, sample 9706-54 m, *Polonodus* sp./*P. horridus* Zone, $\times 125$, 12829/3. (d) Bacterial filaments, incident light, sample 9706-52 m, *Polonodus* sp./*P. horridus* Zone, $\times 20$, 12829/4. (e–g) Lingulid brachiopods, incident light. (e) *Pomeraneotreta* sp., sample 9706-20.3 m, *S. spinatus* Zone, $\times 40$, 12829/5. (g) *Barbatiella?* sp., sample 9706-9 m, *P. proteus* Zone, $\times 34$, 12829/6. (f) Rhabdopleurid? pterobranch fragment, transmitted light, sample 9706-1.5 m, *P. proteus* Zone, $\times 35$, 12829/7. (h) A fragment of caryocaridid shell, transmitted light, sample 9706-18 m, *O. evae* Zone, $\times 25$, 12829/8. (i) 'Cellular' structure on fragments of caryocaridid shell, SEM photomicrographs, sample 9706-18 m, *O. evae* Zone, 12829/9, the scale bar is 50 μm .

elements). The assemblage also includes *P. proteus*, *Tripodus* sp., *D. arcuatus*, *Prioniodus* sp., *Decoriconus peselephantis* (Lindström) and *Oelandodus* sp.

The composition of the assemblage is somewhat different in the sample from 9 m, where *Prioniodus oepiki* McTavish (Figs 8, 9) becomes very abundant. *Paroistodus parallelus* (Pander) is also documented here for the first time. The uppermost sample referred to this zone is poor in conodonts and contains mainly *P. gracilis* elements.

4.b. *Prioniodus elegans* Biozone

This is known from a single sample (14.8 m) and is characterized by the presence of *D. arcuatus*, *D. peselephantis*, *Prioniodus* cf. *P. adami* Stouge & Bagnoli, *Oelandodus* sp. and *P. gracilis*. The latter species is the most abundant, comprising 90% of conodont elements in the sample. Only a single diagnostic element of *Prioniodus elegans* Pander has been found in this particular sample, but it was

observed commonly in some isolated localities of the Burubaital Formation, where it is associated with a similar conodont assemblage.

Oepikodus evae Biozone. This assemblage is known from five samples (16 m, 16.5 m, 18.1 m, 19 m and 19.1 m). It comprises *D. arcuatus*, *P. gracilis*, *Protoprioniodus simplicissimus* McTavish, *Periodon flabellum* (Lindström), *D. peselephantis*, *Protopanderodus* cf. *P. rectus*, *Oelandodus* sp. and *Bergstroemognathus* sp. The nominal species is rare whereas *P. gracilis* remains the most common taxon. *P. flabellum* becomes dominant in the three uppermost samples, where it occurs together with another unidentified species of *Prioniodus*.

4.c. *Spinodus spinatus* Biozone

This is defined by the lowermost occurrence of the nominal species in the sample from 20.3 m. *P. flabellum* remains the most abundant taxon through the whole stratigraphical interval referred to this zone (samples 23 m, 25.1 m, 27.5 m, 32 m and 33.3 m) and usually comprises about 50–70 % of the total number of elements in a particular sample. The two uppermost samples are poor in conodonts but contain an increasing number of *Fahraeusodus marathonsensis* (Bradshaw) elements (up to 30 %). Other components of the conodont fauna are *Protopanderodus* sp., *D. arcuatus*, *P. simplicissimus*, *Ansella longicuspica* Zhang, *P. flabellum*, *Periodon aculeatus* Hadding, *Erraticodon balticus* Dzik and *Tripodus* cf. *laevis* Bradshaw. The latter species, however, is represented by only a few specimens in the lowermost sample of the zone and its identification remains somewhat tentative. *P. aculeatus* and *P. flabellum* commonly occur together in the lower Darriwilian cherts of Kazakhstan (Fig. 7d).

4.d. *Polonodus* sp. Biozone

This is the uppermost biostratigraphical unit in the section (samples 40.5 m, 41.2 m, 45.4 m, 52 m and 54 m). It is defined by the first occurrence of *Polonodus* sp. and *Paroistodus horridus* Barnes & Poplawski in the section. Other conodont species include *A. longicuspica*, *Histiodella holodentata* Ethington & Clark, *P. aculeatus*, *Protopanderodus* sp. and *D. arcuatus*. A few elements of *Nordiora* are also recorded (Fig. 7i).

5. Other components of the faunal assemblages

Radiolarians, the primary sediment-producing organisms, are abundant in all varieties of cherts exposed in the section, but they are often affected or destroyed by diagenetic dissolution in the middle part of individual beds and are usually better preserved close to the bedding surfaces of chert layers. Their concentrations accentuate fine lamination, which is disrupted occasionally by bioturbation. Radiolarians are also better

preserved in rocks of an intensive red colour than in the lighter coloured cherts, where radiolarian opal is usually completely recrystallized or occasionally replaced by iron oxides (Fig. 5b, c).

Spicules of hexactinellide sponges (mainly monaxon and tetraxon forms) represent another source of siliceous bioclasts in the rock (Fig. 5a). They are usually more abundant and better preserved near the bedding surfaces and almost disappear towards the middle part of individual beds. However, this stratification is more probably related to a degree of secondary silica recrystallization in chert layers and does not reflect primary distribution of bioclasts in the rock.

Lingulate brachiopods are relatively common only in the Darriwilian interval of the succession (18–25.1 m). They are represented by micromorphic linguloids and acrotretoids including *Barbatulella?* sp., *Pomeraniotreta* sp. and two or three other unidentified genera (Fig. 5e, g).

Caryocaridids are usually represented by small fragments of carapaces (from 1 mm to 5 mm) with a preserved cell-like structures (Fig. 5i). The cellular structure of all fragments is almost identical. ‘Cells’ are elongated, approximately 20 micrometers in length. The margins of some plates possess conical spines, which are commonly preserved on their terminal ends (Fig. 5h). These arthropod remains are very numerous in all varieties of chert, but their preservation is very fragmentary.

Pterobranchs usually occur as small and poorly preserved fragments of colonies (Fig. 5f). Red varieties of cherts in the Darriwilian interval are rich in bacterial filaments varying greatly in size and are chaotically oriented (Fig. 5d).

6. Discussion

The Ordovician Period was characterized by extensive sedimentation of biogenic siliceous deposits, which are represented mostly by radiolarites and on a much lesser scale by spongiolites (for review, see Racki & Cordey, 2000). Strongly dislocated remnants of the sedimentary cover of Ordovician oceans are now preserved in ophiolite assemblages and subduction–accretion complexes formed along the Palaeozoic active margins of Laurentia (Danelian & Floyd, 2001; Ganis, Williams & Repetski, 2001), Baltica (Savelieva *et al.* 1997), and East Gondwana (Miller & Gray, 1996; Murray & Stewart, 2001; Robertson & Collins, 2001) or are associated with complex tectonic collages of Kazakhstan (Zhylkaidarov, 1998; Tolmacheva, Danelian & Popov, 2001; Dubinina, 1991), Central Asia (Volkova & Budanov, 1999) and Alaska (Dumoulin *et al.* 1997). Records of conodont occurrences from these kinds of sediments leave little doubt that these animals were among the most important components of the pelagic biota in Ordovician oceans, however, existing data remain sparse and incomplete (for

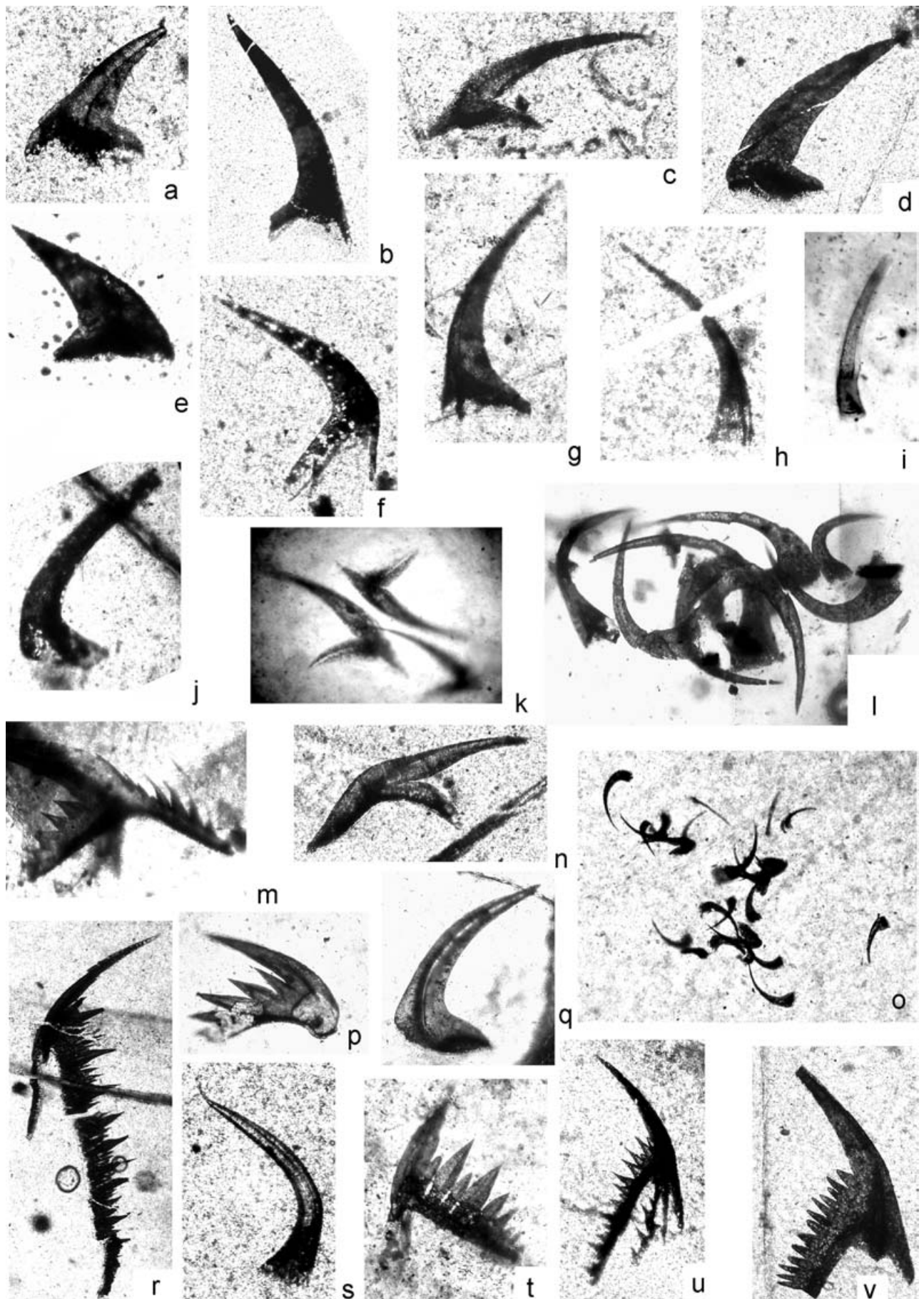


Figure 6. For legend see facing page.

references, see Lamont & Lindström, 1958; Iwata *et al.* 1995; Popov & Tolmacheva, 1995; Zhylykaidarov, 1998; Floyd, 2001; Murray & Stewart, 2001; Dubinina, 1998; Lyons & Percival, 2002). The majority of the reported oceanic conodont faunas contain species that were previously supposed to be typical for the North Atlantic conodont province (*P. gracilis*, *Periodon* spp., *Pygodus* spp.).

6.a. North Atlantic affinity of open oceanic conodont faunas

Global palaeogeographical reconstructions suggest a location of Kazakhstan in equatorial/subequatorial palaeolatitudes (20° N–20° S) during the Ordovician (Scotese & McKerrow, 1991). The surprising discovery that conodonts from successions of ribbon-banded radiolarian cherts in Kazakhstan are of presumably cold water North Atlantic affinity was usually explained previously by their deep-water habitat below the thermocline level (Dubinina, 1991; Zhylykaidarov, 1998). The majority of conodont taxa, for example, *P. gracilis*, *S. spinatus*, *D. arcuatus*, *O. evae*, *P. horridus*, *F. marathonsensis* and representatives of *Periodon* and *Tripodus* lineages, are commonly documented currently in the offshore peripheral successions of all palaeocontinents, and are not considered as indicators of warm/cold water but as open oceanic and pandemic species (Albanesi & Barnes, 2000; Rasmussen, 1998, 2001).

The close similarity of open oceanic conodont assemblages and conodonts from relatively shallow and cool water successions of palaeocontinents located at high latitudes (e.g. Baltoscandia) might be argued to support the hypothesis of a markedly different thermohaline oceanic circulation system in Ordovician times from that of today (Railsback *et al.* 1990). This inverse thermohaline circulation allows dispersion of shallow and cool water species in open oceanic environments in the photic zone above the thermocline level. Oxygen-depleted warm, saline, deep waters characteristic of this circulation support the formation of organic-rich deposits, which are abundant in the Ordovician, but are relatively rare in modern oceanic sediments.

6.b. Dominant character of conodont assemblages

The strong predominance of a few or a single species, such as *P. gracilis*, *P. flabellum*, *P. aculeatus*, *Pygodus serra* (Hadding) and *P. anserinus*, is a typical feature of Early to Middle Ordovician conodont assemblages from radiolarian cherts reported world-wide (Iwata *et al.* 1995; Murray & Stewart, 2001; Dubinina, 1998). Discovery of a species other than the dominant taxa is relatively rare and in cases when the abundance of conodont elements in the rock is low, the assemblage appears almost monospecific (Danelian & Floyd, 2001). The relative abundance of the above-named taxa in the Burubaital Formation corresponds well with the generally observed pattern. In particular, *P. gracilis* constitutes more than 90 % of the total number of elements in samples 9706–4 m, 10.7 m and 14.8 m, while the abundance of *P. flabellum* (samples 16 m–20 m) is up to 80 % and *P. aculeatus* (samples 32 m–33 m) makes up to 60 % of the total number of elements. However, there are also some intervals where conodont assemblages include three or four dominating species in association with less abundant taxa (Fig. 4). Overall, the conodont assemblages from the Burubaital Formation exhibit no significant differences from the pattern observed in the shallow water carbonates of Baltoscandia, which also show the dominance of a single species in some stratigraphical intervals characterized by abiotic events (Tolmacheva *et al.* 2003).

Our observations also suggest that the apparently monospecific or oligospecific character of conodont assemblages from radiolarian cherts reported elsewhere could be in part a result of selective sampling or a side effect of laboratory treatment. In particular, such taxa as *P. gracilis* or *Periodon* spp. are relatively large and easily recognizable taxa, and they are a primary subject of sampling in the field even if they are not the most numerous in a particular sample.

6.c. Eutrophic oceans

The radiolarian cherts of the Burubaital Formation most probably represent a sedimentary cover of the

Figure 6. Optical photomicrographs (incident light) of thin sections showing conodonts from the *P. proteus*–*S. spinatus* zones. (a–f) *Tripodus* cf. *T. laevis* Bradshaw, sample 9706-20.3 m, *S. spinatus* Zone. (a) Pb element, × 65, 12829/10. (b) Sc element, × 60, 12829/11. (c) M element, × 60, 12829/12. (d) ?Pa element, × 60, 12829/13. (e) Pb elements, × 65, 12829/14. (f) Sd element, × 60, 12829/15. (g, h) *Tripodus* sp. from sample 9706-1.5 m, *P. proteus* Zone. (g) Sb element, × 55, 12829/16. (h) Sa element, × 60, 12829/17. (i) *Decoriconus peselephantis* (Lindström) from sample 9706-9 m, × 80, 12829/18. (j) *Protopanderodus* cf. *P. rectus* (Lindström), sample 9706-9 m × 70, 12829/19. (k) Cluster comprises three elements of *Oelandodus* sp., sample 9706-16.6 m, *O. evae* Zone, × 50, 12829/20. (l) Cluster comprises eight coniform elements of *Drepanodus arcuatus* Pander, sample 9706-19 m, *O. evae* Zone, × 55, 12829/21. (m) *Prioniodus elegans* Pander, Pa element from sample 9706-14.8 m, *P. elegans* Zone, × 65, 12829/22. (n, p) *Paracordylodus gracilis* Lindström from sample 9706-4 m, *P. proteus* Zone. (n) M element, × 70, 12829/23. (p) P element, × 65, 12829/24. (o) Cluster comprises twenty-four elements of *Parioistodus parallelus* (Pander); twenty-one coniform and three geniculate elements, sample 9706-9 m, *P. proteus* Zone. All elements in the cluster are very small and juvenile, × 50, 12829/25. (q) *Parioistodus parallelus* (Pander) from sample 9706-9 m, *P. proteus* Zone, × 65, 12829/26. (r–t) *Oepikodus evae* (Lindström), sample 9706-16 m, *O. evae* Zone. (r) Sb element, × 55, 12829/27. (t) Pa element, × 60, 12829/28. (s) ?*Protopanderodus* sp. from sample 9706-20.3 m, *S. spinatus* Zone, × 60, 12829/29. (u, v) *Prioniodus* cf. *P. adami* Stouge & Bagnoli, sample 9706-18 m, *O. evae* Zone. (u) Sd element, × 55, 12829/30. (v) Sb element, × 65, 12829/31.

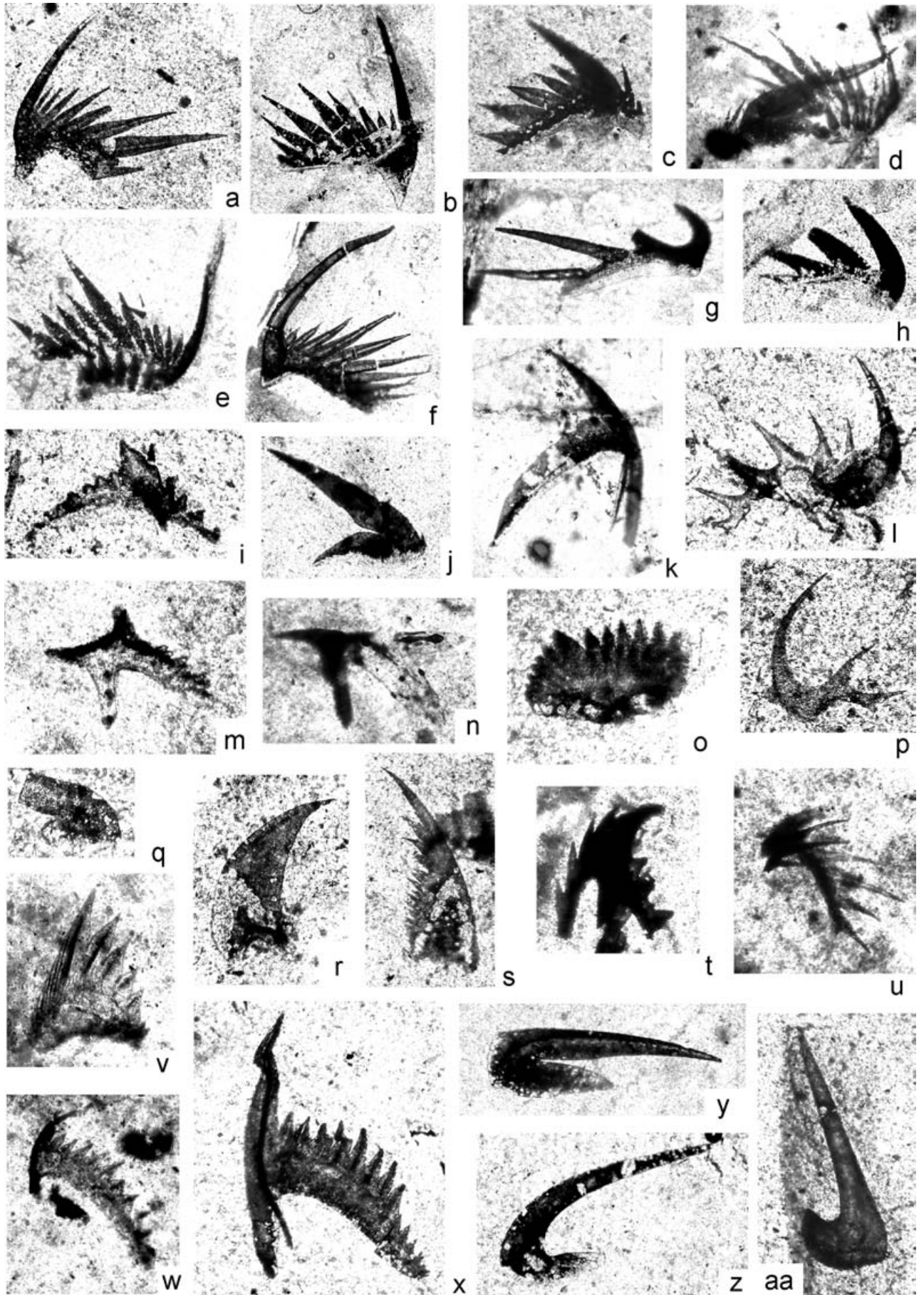


Figure 7. For legend see facing page.

oceanic basement formed in open oceanic environments somewhere between the eastern margin of Baltica and equatorial East Gondwana. These almost pure, biosiliceous sediments are characterized by minor siliciclastic input and were formed far from any source of fine siliciclastic and volcanic material.

The minimum sedimentation rate of radiolarites of the Burubaital Formation, estimated by assuming that continuous deposition completely spanned the Lower Ordovician, was approximately 1.5 m per m.y. This rate of sedimentation is comparable with data on the sedimentation rates of different Mesozoic and Cenozoic ribbon-banded radiolarites (Molinie & Ogg, 1992) and comparable with those from zones of modern accumulations of radiolarian oozes, despite the fact that modern oozes contain a significant siliciclastic input (Sadler, 1981; Schindel, 1980). Radiolarites from another area of Kazakhstan, in the Ushkyzyl Formation (South Predchingsiz Region), are characterized by even thicker (> 120 m) chert successions than those of the Burubaital Formation (Zhylkaidarov, 1998).

The accumulation rates of opal have been often used as a proxy for productivity (e.g. Pokras, 1986) and, as shown recently, high primary productivity of surface seawater and distribution of cherts show positive correlation through the Phanerozoic (Bartolini, Baumgartner & Guex, 1999). By contrast, the accumulation of opal is strongly influenced by dissolution in the water column. Oceanic water in the Ordovician was more highly saturated with silica than Recent oceanic water, which is typically depleted in dissolved silica (Kidder & Erwin, 2001). Significant recrystallization and dissolution of radiolarian shells is observed in the lower part of the section of the Burubaital Formation, most probably induced by increased alkalinity or salinity of the bottom water. Nevertheless, relatively high sedimentation rates of chert deposition in the early to mid-Ordovician of Central Kazakhstan indirectly proves a high primary biological productivity in the basin.

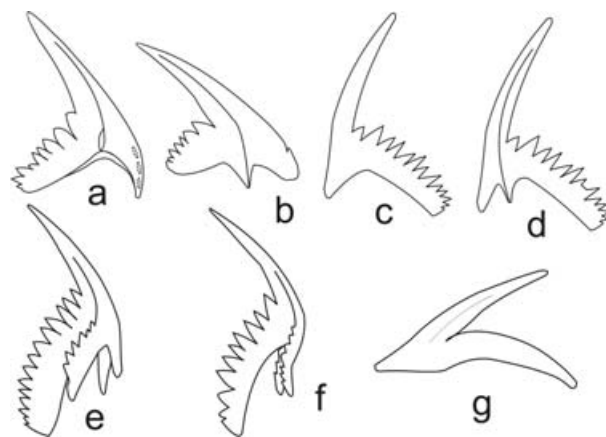


Figure 8. Interpretative drawings of *P. oepiki* (McTavish) elements. (a) Pa element, outer view. (b) Pb element, outer view. (c) Sc element. (d) Sb element, outer view. (e) Sd element. (f) Sa element. (g) M element.

Preservation of defused organic matter in the cherts, the presence of organic films, and of conodont natural assemblages preserved intact in coprolites, are in favour of sluggish water circulation and density stratification, and high fertility of surface waters in the basin during late Cambrian and early to mid-Ordovician times.

At first glance, the ribbon-banded cherts of the Burubaital Formation in the studied section are very similar in lithology through the time interval from Early to Middle Ordovician. The only visible changes are confined to the appearance of distinctive, uneven bedding surfaces bearing numerous macrofurrows and knolls (0.5–2 cm in diameter), and to a predominance of red-coloured cherts in the upper part of the section. Microscopic studies reveal, however, that cherts from the lower and upper part of the section differ much more significantly. The degree of organic matter utilization and oxygenation was relatively low in the lowermost Ordovician (up to *Prioniodus elegans* Zone), but increased significantly from the Tremadocian to the

Figure 7. Optical photomicrographs (transmitted light) of thin sections showing conodonts from the *S. spinatus* Zone and *Polonodus* sp./*P. horridus* Zone. (a–c, e, f, j) *Periodon flabellum* (Lindstrom). (a) Sc element, sample 9706-41.2 m, *Polonodus* sp./*P. horridus* Zone, $\times 65$, 12829/32. (b) Sc element, sample 9706-20.3 m, *S. spinatus* Zone, $\times 60$, 12829/33. (c) Pa element, sample 9706-20.3 m, *S. spinatus* Zone, $\times 70$, 12829/33. (e) Sd? element, sample 9706-20.3 m, *S. spinatus* Zone, $\times 70$, 12829/34. (f) Sc element, sample 9706-23 m, *S. spinatus* Zone, $\times 60$, 12829/35. (j) M element, sample 9706-20.3 m, *S. spinatus* Zone, $\times 60$, 12829/36. (d) M element of *Periodon aculeatus* Hadding and Sd? element of *P. flabellum*, sample 9706-33.3 m, *S. spinatus* Zone, $\times 60$, 12829/37. (g, h) *Spinodus spinatus* (Hadding), sample 9706-25.1 m, *S. spinatus* Zone. (g) Sc element, $\times 50$, 12829/38. (h) P element, $\times 60$, 12829/39. (l, p, y) *Paroistodus horridus* (Barnes & Poplawski), *Polonodus* sp./*P. horridus* Zone. (l) Sc element, sample 9706-41.2 m, $\times 60$, 12829/40. (p) Sc element, sample 9706-40.5 m, $\times 70$, 12829/41. (y) M element, sample 9706-41.2 m, $\times 65$, 12829/42. (z) *Paroistodus* sp., sample 9706-27.5 m, *S. spinatus* Zone, $\times 50$, 12829/43. (i, t) *Nordiora* sp., sample 9706-52 m, *Polonodus* sp./*P. horridus* Zone. (i) Pb element, $\times 95$, 12829/44. (t) Sd element, $\times 110$, 12829/45. (k) *Protoprioniodus simplicissimus* McTavish, sample 9706-18 m, *S. spinatus* Zone, $\times 90$, 12829/46. (m, n) *Polonodus* sp., sample 9706-41.25 m, *Polonodus* sp./*P. horridus* Zone. (m) Pb element, $\times 100$, 12829/47. (n) Pb element, $\times 80$, 12829/48. (o) *Histiodellella* cf. *H. holodentata* Ethington & Clark, sample 9706-52 m, *Polonodus* sp./*P. horridus* Zone, $\times 100$, 12829/49. (q–s) *Ansella longicuspicata* Zhang, sample 9706-52 m, *Polonodus* sp./*P. horridus* Zone. (q) M element, $\times 90$, 12829/50. (r) P element, $\times 90$, 12829/51. (s) S element, $\times 90$, 12829/52. (u) *Erraticodon balticus* Dzik, Sb element, 9706-32 m, $\times 50$, *S. spinatus* Zone, 12829/53. (v–x) *Fahraeusodus marathoniensis* (Bradshaw), sample 9706-32 m, *S. spinatus* Zone. (v) P element, $\times 100$, 12829/54. (w) Sc element, $\times 95$, 12829/55. (x) Sb element, $\times 90$, 12829/56. (aa) *Drepanodus arcuatus* Pander, Pb (pipaform) element from sample 9706-52 m, *Polonodus* sp./*P. horridus* Zone, $\times 70$, 12829/57.

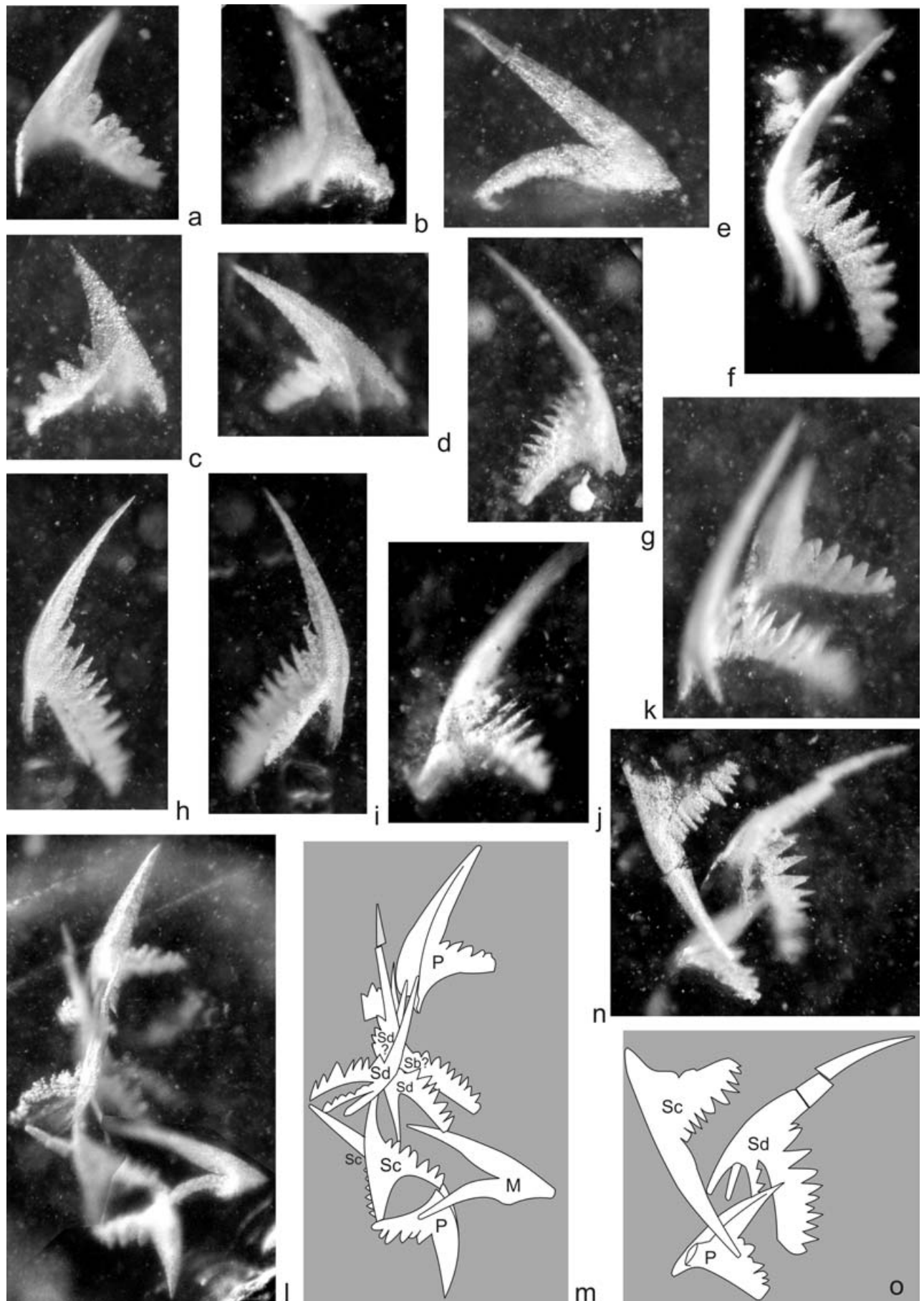


Figure 9. For legend see facing page.

Darriwilian. This is expressed in the disappearance of conodont clusters, in microbioturbation of the sediment, and in the appearance of strongly shredded organic films. The diffused organic matter is characteristic of laminated, black and grey cherts in the Tremadocian part of the sequence, but it almost disappears at higher stratigraphic levels, indicating a well-oxygenated depositional environment, unfavourable for preservation of the organic matter. The 'jasper' structures that are typical for sediments enriched in iron oxides are commonly observed in the Middle Ordovician cherts of the Burubaital Formation.

The cherts of the Ushkyzyl Formation in the Chingiz Mountain Range, eastern Central Kazakhstan generally resemble those of the Burubaital Formation, although these regions are currently located more than 700 km apart (Zhylkaidarov, 1998; Tolmacheva, unpub. data). These contemporaneous radiolarite sediments are comparable in their thickness, in the character of bedding, and in the taxonomic composition of conodont assemblages. Darriwilian radiolarites of the Ushkyzyl Formation also contain rare sponge spicules and nodules on bedding surfaces of individual beds, which were possibly formed during diagenesis (Zhylkaidarov, 1998). Similar variations in chert colours, from grey and white in the Tremadoc to red in the Arenig and Llanvirn (British series), are also characteristic of the Ushkyzyl Formation. This indicates that increased oxygenation of near-bottom waters during the Tremadoc–Arenig transition may represent a widespread phenomenon in the oceanic space between Baltica and equatorial East Gondwana. It may reflect significant changes of characters of oceanic circulation and in primary productivity.

7. Conclusions

Recent studies of Early Palaeozoic pelagic faunal assemblages are confined mostly to the margins of major continents and ancient volcanic arcs, whereas the characters of the pelagic biota from oceanic sediments remain mostly unknown. Diverse fossil assemblages have been documented from the Ordovi-

cian ribbon radiolarites of the Burubaital Formation in Central Kazakhstan. These biosiliceous sediments were deposited in basinal environments, inhabited by lingulate brachiopods, sponges, pterobranchs and unidentified arthropods. A continuous succession of conodont biozones from the upper Cambrian to the Middle Ordovician (lower Darriwilian) is preserved in the siliceous sediments of this formation. Our interpretation is that these radiolarites were deposited in open oceanic environments characterized by high fertility and primary productivity of surface waters.

The North Atlantic Province affinity of the oceanic conodont fauna in Kazakhstan, typical elsewhere of shallow, cool water epicratonic basins located in temperate latitudes (e.g. Baltica and South China), could support the hypothesis of a reversed thermohaline oceanic circulation system in the Ordovician by comparison with today. A significant increase in oxygenation of bottom waters is documented near the Tremadoc/Arenig (British series) boundary, and this shift was probably regional and related to a change in palaeo-oceanographical circulation patterns.

The structure of the open oceanic conodont assemblages is no different in general from that of shallow water environments, which also often exhibit the dominance of a single species.

8. Systematic palaeontology

Family Prioniodontidae Bassler, 1925

Genus *Prioniodus* Pander, 1856

Type species. Prioniodus elegans Pander, 1856.

Prioniodus oepiki (McTavish)

Figure 8a–g; Figure 9a–o

- 1973 *Baltoniodus oepiki* sp. nov. McTavish, pp. 43–4 (*partum*), pl. 2, figs 1, 10, 12, 13 (only), text–figs 4b–c, 6o.
- 1973 *Acodus emanuelensis* sp. nov. McTavish, pp. 40–1 (*partum*), pl. 2, fig. 20 (only).
- ?1973 *Baltoniodus* aff. *B. triangularis* (Lindström); McTavish, p. 44 (*partum*), pl. 2, fig. 7, text–fig. 4a

Figure 9. Optical photomicrographs (incident light) of elements of *P. oepiki* (McTavish) and drawings of the element clusters preserving partial apparatuses of *P. oepiki*. All elements and clusters are from the sample 9706-9 m, Burubaital Formation, West Balkhash Region, Central Kazakhstan, *P. proteus* Zone, Tremadoc. (a) Pa element, inner view, $\times 75$, 12829/58. (b) Pa element, outer view, $\times 80$, 12829/59. (c) Pb element, outer view, $\times 70$, 12829/60. (d) Pb element, outer view, $\times 70$, 12829/61. (e) M element, $\times 80$, 12829/62. (f) Sa element, $\times 90$, 12829/63. (g) Sb element, outer view, $\times 85$, 12829/64. (h) Sd element, inner view, $\times 85$, 12829/65. (i) Sd element, outer view of the element illustrated in Figure 8h: $\times 85$, 12829/66. (j) Sc element, $\times 80$, 12829/67. (k) Element cluster comprises one Pa element and one Sb element, $\times 85$, 12829/68. (l) Element cluster, $\times 80$, 12829/69. (m) Interpretative drawing of specimen 12829/69 shown in (l). Cluster comprises one Pa element, one Pb element, one M element, two Sc elements, two Sd elements and two S elements. The morphology of the two latter S elements is difficult to recognize because of their overlapped position in the cluster. (n) Element cluster, holotype, $\times 75$, 12829/70. (o) Interpretative drawing of specimen 12829/70 shown in (n). Cluster comprises one Pa element, one S element and one Sd element.

- 1988 *Prioniodus oepiki* (McTavish); Stouge & Bagnoli, pp. 135–6 (*partum*), pl. 12, figs 1–3, 6–11 (only).
- 2001 *Prioniodus oepiki* (McTavish); Ganis, Williams & Repetski, fig. 12, J–M, P, B' (only).

Emended diagnosis. A species of *Prioniodus* consisting of septimembrate apparatus with ramiform–pectiniform structure. Both Pa and Pb elements with denticulate processes; M elements with adenticulate anterior extension of the base; S elements with large basal sheath, deep basal cavity and denticulate posterior processes; Sa elements with denticles on both lateral processes and Sd elements bearing denticulate outer processes and adenticulate inner lateral processes.

Description. Pa element has a thick, keeled, slightly reclined cusp and denticulate anterior processes which are relatively long and strongly curved inward. The lateral processes of the majority of specimens are short and adenticulate, but a few gerontic Pa elements bear one to two small denticles on the lateral processes. The anterior process usually has four to six small, reclined denticles. The posterior process has four to six straight or slightly reclined denticles, usually thicker and coarser than those ones of S elements. Cusp is relatively short and thick, compressed laterally and keeled. Basal cavity is deep with a large basal sheath. Pb element has a thick, slightly reclined cusp and a base with short posterior, anterior and lateral processes; the latter one is usually adenticulate. Denticles on the posterior process are relatively large, straight and compressed, about five to eight in number. Anterior process is projected anteriorly or slightly turned inward, usually with one to four small reclined denticles. Lateral process is shorter than that of Pa elements. Most of the specimens in the collection are characterized by adenticulate lateral processes, however, there are a few gerontic specimens bearing two denticles on the lateral processes. Basal cavity is deep with a large basal sheath. Sc element has a short adenticulate anticus and a long posterior process slightly curved aborally. Both lateral sides of the element are usually smooth or with flat median carina on the outer one. Denticles on posterior process are straight and usually of about equal size.

Sb element has a large basal sheath, a long posterior process, an adenticulate short anticus and a keel on the outer lateral side of the element extending slightly beyond the basal margin as a short adenticulated process. The posterior process, straight or slightly turned downward, has straight, well-developed denticles of approximately equal sizes.

Sd element is characterized by a long adenticulate anticus and two lateral processes; outer one is denticulate. The posterior process is slightly curved aborally and bears relatively large, straight denticles of about equal size. Outer lateral process is long, bearing well-

developed, minute denticles. Inner lateral processes of the adult specimen are usually twice as small as the outer lateral processes and always adenticulate.

Sa element has two denticulate processes, which bear small denticles. Posterior process is turned slightly downward. Lateral processes are long and are more than half the length of the posterior process of the adult elements. Denticles on the posterior process are erect and regular, whereas denticles on the lateral process are small and slightly inclined towards the cusp. The number of denticles on adult specimens ranges from five to eight.

M element is oistodiform with a prominent, strongly reclined cusp and a short adenticulate anticus. Oral edge of base is long, keeled and adenticulate. It joins with the posterior keels of the cusp at an angle of about 45 degrees. Basal cavity is relatively deep. Aboral margin has a small bulge.

Description of clusters. Three incomplete clusters of *P. oepiki* elements have been found in the sample from unit 2 (9 m). Specimen 12829/69 (Fig. 9l, m) is an incomplete cluster that comprises nine elements: one Pa element, one Pb element, two Sc elements, one Sd element, one M element and three unidentified S elements. More precise identification of latter S elements is impossible because of their overlapped position in the cluster. The arrangement of elements in the cluster retains in part their original position near the axis of apparatus: S elements are situated in the middle of the clusters, whereas P elements and M element are positioned at the margins of the cluster. All elements are relatively small and probably juvenile. The specimen does not represent a full number of elements within the *Prioniodus* apparatus, however, it preserves partly the original orientation of the elements and nicely illustrates the element types comprising the multi-elemental apparatuses of *P. oepiki*.

Cluster 12829/70 (Fig. 9n, o) comprises three elements: Sc, Sd and Pa elements. All elements in the cluster are large and their morphology is easily recognizable. Specimen 12829/68 (Fig. 9k) is represented by a pair of aligned Pa and Sb elements.

The largest cluster 12829/69 comprises elements of about equal sizes, whereas P elements of the other two clusters are smaller than the corresponding S elements. An observation of the element proportions in these three clusters suggests that P elements increase their size during growth, whereas P elements in *P. oepiki* apparatuses exhibit slightly negative allometry during ontogeny.

Remarks. *P. oepiki* was recorded from three continents besides Kazakhstan: from the Cow Head Peninsula sections of western Newfoundland (Stouge & Bagnoli, 1988), from the Emanuel Formation of Western Australia (McTavish, 1973) and from Hamburg klippe in Pennsylvania (Ganis, Williams & Repetski, 2001). In all of these reports, M elements bearing small

denticles on the anterior side of the anticusp were suggested to be the M element of *P. oepiki*. However, the M element found in cluster together with P and S elements of *P. oepiki* is completely different from that depicted by McTavish (1973) and others in having the adenticulate short anterior extension of the base. This adenticulate M element closely resembles the M element assigned to the *Acodus emanuelensis* McTavish (McTavish, 1973); the latter is considered to be an M element of *P. oepiki*.

In Kazakhstan *P. oepiki* has a narrow stratigraphical interval of distribution restricted to the upper part of the *P. proteus* Zone, however, its geographical distribution is wide; it was documented from several isolated localities and sections of the Burubaital (Tolmacheva & Purnell, 2002) and the Ushkyzyl Formation in the Chingiz Mountain Range (Tolmacheva, unpub. data).

Geographical and stratigraphical occurrence. Upper part of *P. proteus* Zone, Burultas Tectonofacies Belt and Chingiz Mountain Range, Central Kazakhstan.

Material. Pa elements – 8; Pb elements – 5, Sc elements – 6, Sb elements – 6, Sd elements – 10; Sa elements – 3; M elements – 7; three natural assemblages of elements comprising nine, three and two elements.

Acknowledgements. T. Tolmacheva, L. Holmer and L. Popov gratefully acknowledge financial support from the Swedish Research Council (VR), the Wenner-Gren Center Foundation, the Royal Swedish Academy of Sciences (KVA). Fieldwork was also made possible with the financial support of the National Museum of Wales, Cardiff. The studies of T. Tolmacheva and I. Gogin were financed partly by RFFI (Russian Foundation of Fundamental Investigations) grant no. 02 05–64 775. We are grateful to M. G. Bassett and both reviewers for constructive comments on the manuscript.

References

- AITCHISON, J. C. 1998. A new Lower Ordovician (Arenigian) radiolarian fauna from the Ballantrae Complex, Scotland. *Journal of Scottish Geology* **34**, 73–81.
- ALBANESI, G. L. & BARNES, C. R. 2000. Subspeciation within a punctuated equilibrium evolutionary event: Phylogenetic history of the lower-Middle Ordovician *Paroistodus originalis*–*Phorridus* complex (Conodonta). *Journal of Paleontology* **74**, 492–502.
- ANTONYUK, R. M. 1974. Proterozoi i nizhnii kembrii vostoka tsentralnogo Kazakhstana. [Proterozoic and Lower Cambrian of eastern Central Kazakhstan.] In *Dopaleozoi i paleozoi Kazakhstana. 1. Stratigrafiya kembriya, ordovika i silura Kazakhstana* (ed. A. A. Abdulin), pp. 67–73. Alma-Ata: Nauka.
- APOLLONOV, M. K. 2000. Geodinmicheskaya evolyutsiya Kazakhstana v rannem paleozoe s pozitsiyi klasicheskoi tektoniki plit. [Geodynamic evolution of Kazakhstan in the Early Palaeozoic (from classic plate tectonic positions).] In *Geodinamika i minerageniya Kazakhstana* (ed. H. A. Bespaev), pp. 46–63. Almaty: VUC Publishing House.
- BARTOLINI, A., BAUMGARTNER, P. O. & GUEx, J. 1999. Middle and Late Jurassic radiolarian palaeoecology versus carbon-isotope stratigraphy. *Palaeogeography, Palaeoclimatology, Palaeoecology* **145**, 43–60.
- BASSLER, R. S. 1925. Classification and stratigraphic use of the conodonts. *Bulletin of the Geological Society of America* **36**, 218–20.
- DANELIAN, T. & FLOYD, J. 2001. Progress in describing Ordovician siliceous biodiversity from the Southern Uplands (Scotland, U.K.). *Transactions of the Royal Society of Edinburgh Earth Sciences* **91**, 489–98.
- DUBININA, S. V. 1991. Upper Cambrian and Lower Ordovician conodont associations from open ocean paleoenvironments, illustrated by Batyrbay and Sarykum sections in Kazakhstan. In *Advances in Ordovician geology* (eds C. R. Barnes and S. H. Williams), pp. 107–24. Geological Survey of Canada, Paper 90-9. Ottawa.
- DUBININA, S. V. 1998. Conodonts from the Early Ordovician (mid-Arenig) deep-water deposits of central Asian paleobasins. *Palaeontologia Polonica* **58**, 79–86.
- DUGDALE, R. C. & WILKERSON, F. P. 1998. Silicate regulation of new production in the equatorial Pacific upwelling. *Nature* **391**, 270–3.
- DUMOULIN, J. A., BRADLEY, D. C., HARRIS, A. G. & REPETSKI, J. E. 1997. *Lower Palaeozoic deep-water facies of the Medfra Area, Central Alaska*. United States Geological Survey Professional Paper 1614, 73–103.
- DVOICHENKO, N. K. & ABAIMOVA, G. P. 1987. Konodonty i biostratigrafiya vulkanogenno-kremnistykh tolsch Tcentral'nogo Kazakhstana. [Conodonts and biostratigraphy of volcanic and siliceous strata of the Lower Palaeozoic of Central Kazakhstan]. In *Microfauna and biostratigraphy of the Phanerozoic of Siberia and adjacent areas*, pp. 160–78. Institute of Geology and Geophysics, Academy of Science USSR, Siberian branch, Trudy, 651. Novosibirsk: 'Nauka'.
- FLOYD, J. D. 2001. The Southern Uplands Terrane; a stratigraphic review. In *The Southern Uplands Terrane; tectonics and biostratigraphy within the Caledonian Orogen; proceedings* (eds E. N. K. Clarkson, J. D. Floyd and P. Stone), pp. 349–62. *Transactions of the Royal Society of Edinburgh, Earth Sciences* **91**.
- GANIS, G. R., WILLIAMS, S. H. & REPETSKI, J. E. 2001. New biostratigraphic information from the western part of the Hamburg klippe, Pennsylvania, and its significance for interpreting the depositional and tectonic history of the klippe. *Bulletin of the Geological Society of America* **113**, 109–28.
- GRIDINA, N. M. & MASHKOVA, T. V. 1975. Konodonty v terrigenno-kremnistykh tolschakh Atasuisikogo anticlinoria. [Conodonts from siliciclastic and siliceous deposits of the Atasuisikii anticlinoria.] *Isvestia Akademii Nauk KazSSR, Alma-Ata* no. 6, 47–8.
- HOLMER, L. E., POPOV, L. E., KONEVA, S. P. & BASSETT, M. G. 2001. Cambrian–Early Ordovician brachiopods from Malý Karatau, the western Balkhash Region, and northern Tien Shan, Central Asia. *Special Papers in Palaeontology* **65**, 180 pp.
- IWATA, K., SCHMIDT, B. L., LEITCH, E. C., ALLAN, A. D. & WATANABE, T. 1995. Ordovician microfossils from the Ballast Formation (Girilambone Group) of New South Wales. *Australian Journal of Earth Sciences* **42**, 371–6.
- KIDDER, D. L. & ERWIN, D. H. 2001. Secular distribution of biogenic silica through the Phanerozoic: Comparison of silica-replaced fossils and bedded cherts at the series level. *Journal of Geology* **109**(4), 509–22.

- KOREN, T. N., LYTOCHKIN, V. N., POPOV, L. E. & TOLMACHEVA, T. JU. 1993. *Biostratigraficheskii analiz pelagicheskikh strukturno-veshchestvennykh kompleksov paleozoya dlya tselei GSR-50 i-200*. [Biostratigraphic analysis of the Paleozoic pelagic sedimentary rocks in geologically complicated areas for the purposes of the geological mapping (1:50000 and 1:200000 scale).] St. Petersburg: VSEGEI, 79 pp.
- KURKOVSKAYA, L. A. 1985. Kompleksy konodontov iz kremnistykh I vulkanogenno-kremnistykh tolsch ordovika Tsentral'nogo Kazakhstana. [Conodont assemblages from the siliceous and siliceous-volcanic rocks of the Ordovician of Central Kazakhstan.] In *Geology of the early geosynclinal assemblages of Central Kazakhstan* (ed. Yu. A. Zaitchev), pp. 164–77. Materials on the geology of Central Kazakhstan v. 20. Moscow University.
- LAMONT, A. & LINDSTRÖM, M. 1958. Arenigian and Llandeilian cherts identified in the Southern Uplands of Scotland by means of conodonts, etc. *Edinburgh Geological Society Transactions* **17**, 60–70.
- LÖFGREN, A. 1978. Arenigian and Llanvirnian conodonts from Jämtland, northern Sweden. *Fossils and Strata* **13**, 1–129.
- LYONS, P. & PERCIVAL, I. G. 2002. Middle to late Ordovician age for the Jindalee Group of the Lachlan Fold Belt, New South Wales: conodont evidence and some tectonic implications. *Australian Journal of Earth Sciences* **49**, 801–8.
- MCTAVISH, R. A. 1973. Prioniodontacean Conodonts from the Emanuel Formation (Lower Ordovician) of Western Australia. *Geologica et Palaeontologica* **7**, 27–51.
- MILLER, J. MCL. & GRAY, D. R. 1996. Structural signature of sediment accretion in a Paleozoic accretionary complex, southeastern Australia. *Journal of Structural Geology* **18**, 1245–58.
- MOLINIE, A. J. & OGG, J. G. 1992. Milankovitch cycles in Upper Jurassic and Lower Cretaceous radiolarites of the equatorial Pacific: spectral analysis and sedimentary rate curves. In *Proceedings of the Ocean Drilling Program, Scientific Results, vol. 129* (eds R. L. Larson, Y. Lancelot *et al.*), pp. 529–47. College Station, Texas.
- MURRAY, S. L. & STEWART, I. R. 2001. Paleogeographic significance of Ordovician conodonts from the Lachlan fold belt, southeastern Australia. *Historical Biology* **15**, 145–70.
- NIKITIN, I. F. 2002. Ordovikskie kremniste i kremnisto-bazaltovyye komplekсы Kazakhstana. [Ordovician siliceous and siliceous-basaltic complexes of Kazakhstan.] *Geologiya i Geofizika* **43**, 512–27.
- NIKITIN, I. F., APOLLONOV, M. K. & TSAY, D. T. 1980. O vozraste kremnistykh tolsch niznego paleozoya Yugo-Zapadnogo Pribalkhashiya. [On the age of the siliceous deposits of the lower Palaeozoic of South-West Pribalkhashie.] *Izvestiya Akademii Nauk Kazakhskoi SSR, seriya geologicheskaya* **3**, 42–50.
- NIKITIN, I. F., APOLLONOV, M. K., TSAY, D. T. & RUKAVISHNIKOVA, T. B. 1980. Ordovikskaya sistema. [Ordovician System.] In *Chu-Iliiskii rudnyi poyas. Part 1. Geologiya Chu-Iliiskogo regiona* (ed. A. A. Abdulin), pp. 44–78. Alma-Ata: 'Nauka'.
- NOVIKOVA, M. Z., GERASIMOVA, N. A. & DUBININA, S. V. 1983. Konodonty iz vulkanogenno-kremnistogo kompleksa Severnogo Pribalkhash'ya. [Conodonts of volcanogenic-silicate complexes in northern Balkhash.] *Doklady Akademii Nauk SSSR* **271**, 1449–50.
- PANDER, C. H. 1856. *Monographie der fossilen Fische des Silurischen Systems der russisch-baltischen Gouvernements*. St. Petersburg: Akademie der Wissenschaften, 91 pp.
- POKRAS, E. M. & MOLFINO, B. 1986. Oceanographic control of diatom abundances and species distributions in surface sediments of the tropical and southeast Atlantic. *Marine Micropaleontology* **10**, 165–88.
- POPOV, L. E., COCKS, L. R. M. & NIKITIN, I. F. 2002. Upper Ordovician brachiopods from the Anderken Formation, Kazakhstan: their ecology and systematics. *Bulletin of the British Museum (Natural History), Geology Series* **58**, 13–79.
- POPOV, L. E. & TOLMACHEVA, T. YU. 1995. Conodont distribution in a deep-water Cambrian-Ordovician boundary sequence from south-central Kazakhstan. In *Ordovician Odyssey: short papers for the Seventh International Symposium on the Ordovician System* (eds J. D. Cooper, M. L. Droser and S. C. Finney), pp. 121–4. Fullerton, California.
- RACKI, G. & CORDEY, F. 2000. Radiolarian palaeoecology and radiolarites: Is the present the key to the past? *Earth Science Reviews* **52**, 83–120.
- RAILSBACK, L. B., ACKERLY, S. C., ANDERSON, T. F. & CISNE, J. L. 1990. Palaeontological and isotope evidence for warm saline deep waters in Ordovician oceans. *Nature* **343**, 156–9.
- RASMUSSEN, J. A. 1998. A reinterpretation of the conodont Atlantic Realm in the late Early Ordovician (early Llanvirn). In *Proceedings of the Sixth European conodont symposium (ECOS VI)* (ed. H. Szaniawski), pp. 67–77. *Palaeontologia Polonica* **58**.
- RASMUSSEN, J. A. 2001. Conodont biostratigraphy and taxonomy of the Ordovician shelf margin deposits in the Scandinavian Caledonides. *Fossils and Strata* **48**, 1–180.
- ROBERTSON, A. H. F. & COLLINS, A. S. 2001. Shyok Suture Zone, N Pakistan: Late Mesozoic–Tertiary evolution of a critical suture separating the oceanic Ladakh Arc from the Asian continental margin. *Journal of Asian Earth Sciences* **20**, 309–51.
- SADLER, P. M. 1981. Sediment accumulation rates and the completeness of stratigraphic sections. *Journal of Geology* **89**, 569–84.
- SAVELIEVA, G. N., SHARASKIN, A. YA., SAVELIEV, A. A., SPADEA, P. & GAGGERO, L. 1997. Ophiolites of the southern Uralides adjacent to the East European continental margin. *Tectonophysics* **276**, 117–37.
- SCHINDEL, D. E. 1980. Microstratigraphic sampling and the limits of paleontologic resolution. *Paleobiology* **6**, 408–26.
- SCOTESE, C. R. & MCKERROW, W. S. 1991. Ordovician plate tectonic reconstructions. In *Advances in Ordovician Geology* (eds C. R. Barnes and S. H. Williams), pp. 271–82. Geological Survey of Canada, Paper 90-9. Ottawa.
- STOUGE, S. & BAGNOLI, G. 1988. Early Ordovician conodonts from Cow Head Peninsula Western Newfoundland. *Palaeontographia Italica* **75**, 89–179.
- TOLMACHEVA, S. G., KUZNECHEVSKII, A. G. & PALETCH, L. M. 1974. Stratigrafia. In *Geologiya i metalogeniya Sarytumskoj Zony (Zapadnoe Pribalkhashie)*. [Geology and metalogeny of Sarytuma Zone (West Balkhash region).] (ed. Yu. I. Kazanin), pp. 8–29. Alma-Ata: Nauka.

- TOLMACHEVA, T. & LÖFGREN, A. 2000. Morphology and paleogeography of the Ordovician conodont *Paracordylodus gracilis* Lindström, 1955: Comparison of two populations. *Journal of Paleontology* **74**, 1114–21.
- TOLMACHEVA, T. YU., DANELIAN, T. & POPOV, L. E. 2001. Evidence for 15 m.y. of continuous deep-sea biogenic siliceous sedimentation in early Palaeozoic oceans. *Geology* **29**, 755–8.
- TOLMACHEVA, T. YU., EGERQUIST, E., MEIDLA, T., TINN, O. & HOLMER, L. 2003. Faunal composition and dynamics in unconsolidated sediments: a case study from the Middle Ordovician of the East Baltic. *Geological Magazine* **140**, 31–44.
- TOLMACHEVA, T. & PURNELL, M. 2002. Apparatus composition, growth, and survivorship of the Lower Ordovician conodont *Paracordylodus gracilis* Lindström, 1955. *Palaeontology* **45**, 209–28.
- VOLKOVA, N. I. & BUDANOV, V. I. 1999. Geochemical discrimination of metabasalt rocks of the Fan-Karategin transitional blueschist/greenschist belt, South Tianshan, Tajikistan: Seamount volcanism and accretionary tectonics. *Lithos* **47**, 201–16.
- ZHANG, J. 1998. Conodonts from the Guniutan Formation (Llanvirnian) in Hubei and Hunan provinces, south-central China. *Stockholm Contributions in Geology* **46**, 161 pp.
- ZHYLKAIDAROV, A. 1998. Conodonts from Ordovician ophiolites of central Kazakhstan. *Acta Palaeontologica Polonica* **43**, 53–68.